

# Mechanical Behavior of Nafion<sup>®</sup> and BPSH Membranes

Steven A. Kyriakides

*Virginia Polytechnic Institute and State University  
Department of Materials Science & Engineering  
213 Holden Hall, Virginia Tech  
Blacksburg, Virginia 24061*

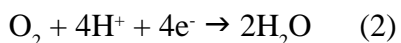
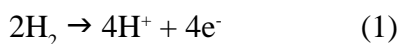
**Keywords**  
mechanical behavior,  
Nafion<sup>®</sup>, BPSH

## Abstract

A brief characterization of the mechanical behavior of Nafion<sup>®</sup> 117 and BPSH-35 membranes took place through uniaxial loading, stress relaxation, and creep compliance tests. Membranes were subjected to uniaxial loading at various strain rates to observe yield and fracture behavior. Stress relaxation tests measured relaxation response to strain rate and relaxation strain. Creep compliance tests led to the formation of a creep master curve for the Nafion<sup>®</sup> membrane. Tests showed that for Nafion<sup>®</sup>, higher strain rates produced higher yield stresses and yield strains as well as faster initial relaxation. Strain rate had no effect on strain at fracture. Higher relaxation strains also led to faster initial stress relaxation in both Nafion<sup>®</sup> and BPSH. BPSH results showed no yield trends in uniaxial loading, though they illustrated lower breaking strains with higher strain rates.

## 1. Introduction

Polymer electrolyte membrane (PEM) fuel cell research currently comprises a large portion of the search for alternatives to combustion engines.<sup>[1-7]</sup> Whereas combustion engines require combustion to convert chemical energy, these cells convert chemical energy directly to electrical energy via the following reactions:



In PEM fuel cells, these reactions take place within the membrane electrode assembly (MEA), which consists primarily of a catalyst-coated polymer membrane, a cathode electrode, and an anode electrode. Hydrogen, either provided in pure form or extracted from another fuel, flows in on one side of the MEA. External air provides oxygen for the other side. The

catalyst coatings, usually platinum, become an anode-cathode pair during the operation of the cell, with the reaction in Equation 1 taking place at the anode and that in Equation 2 taking place at the cathode. The flowing of the electrons produced from the anode reaction provides the electrical energy. The protons can pass through the polymer, at which point they combine with the oxygen and electrons to form water. This water, though a much more environmentally friendly byproduct than those produced by combustion engines, can lead to the failure of the entire fuel cell.

The polymers used for these fuel cells pose a problem in that they will absorb some of the water produced during operation. This saturation alters the properties of the polymer, causing it to swell and produce compressive forces within the membrane. Prolonged swell-

ing initiates relaxation within the polymer. When the fuel cell stops running, the membrane will dry and contract, creating tensile stresses that lead to pinhole ruptures in the polymer. These pinholes effectively destroy the MEA, allowing the hydrogen and oxygen to interact freely without producing electrical energy.

Testing and analyzing the mechanical behavior of these membranes enables improved prediction and understanding of their failure mechanisms. The polymers studied in this project were the popular Nafion® 117, manufactured by DuPont, and BPSH, a potential direct methanol fuel cell alternative to Nafion® supplied by Dr. James McGrath of Virginia Tech.

Mechanical property tests were performed to measure tensile strength and stress relaxation patterns as a function of different strain rates. A dynamic mechanical analyzer (DMA) measured the creep compliance as a function of temperatures and the storage modulus as a function of frequency. Analysis of these results shows the membranes' responses to conditions within fuel cells at different stages of operation and fuel cell life.

## 2. Experimental Procedure

### 2.1 Materials

The Nafion® 117 (N117) extruded films had an equivalent weight (EW) of 1100 and a nominal thickness of 0.007 in. The BPSH-35 (BPSH) membrane had an EW of 770 and a nominal thickness of 0.005 in. Hydrosize Technologies, Inc. made the BPSH particles, which required dissolving, casting, and acidification to create the film and prepare it for testing. This material was completely amorphous at the onset of testing. Fuelcellstore.com sold the extruded N117 films, which required only acidification for testing. The extruded N117 is a semi-crystalline polymer, with the crystallinity dependent on the equivalent weight.<sup>[8]</sup>

### 2.2 Uniaxial Loading

Uniaxial loading tests were performed with samples prepared according to Figure 1 on an Instron 4468 Universal Testing Machine with a 1kN load cell.

Pneumatic grips held the 10mm segments at each end of the sample in the Instron machine under a 3 kg/cm<sup>2</sup> force. Strips of white reflective tape,

represented by the lines across the sample, created an extensometer gauge length of 10 mm. A Fiedler Optoelektronik GmbH laser extensometer measured the extension between the strips of tape. The partially reflective surface of the N117 produced some noise

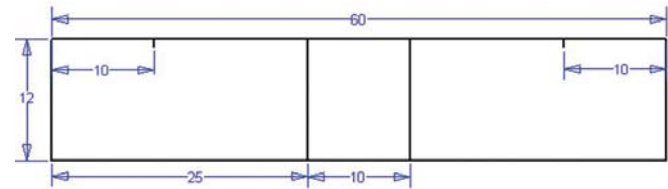


Figure 1. Uniaxial test samples (all dimensions in mm)

in the extensometer's results. The BPSH was so reflective that the extensometer could not differentiate between the membrane and the tape strips. Instead, the Instron machine's crosshead displacement was used to determine the BPSH extension. Samples underwent loading at strain rates of 0.025, 0.07, 0.12, 0.3, and 0.7 min<sup>-1</sup>. Testing consisted of at least three N117 replicates for each strain rate and at least one BPSH replicate per strain rate.

### 2.3 Creep Compliance

Creep compliance tests were conducted using two TA Instruments 2980 Dynamic Mechanical Analyzers (DMA) using 6.5 by 26mm samples. With a preload force of 0.1 N and a stress of 0.5 MPa for N117 and 1.0 MPa for BPSH, the DMA measured creep compliance for two hours and the recoverable compliance for the subsequent two hours. The temperatures used for the N117 tests ranged from 10°C to 130°C in 10°C increments. BPSH test temperatures ranged from 150°C to 230°C, also in 10°C increments.

## 3. Results and Discussion

### 3.1 Uniaxial Loading

Figure 2 displays some of the results of the N117 uniaxial loading tests. This figure illustrates rising yield stresses and decreasing yield strains with increasing strain rate. This information, verified below in Table 1, agrees with the behavior described by Brown.<sup>[9]</sup> The Young's modulus for N117 remained roughly constant at 258 ± 8 MPa.

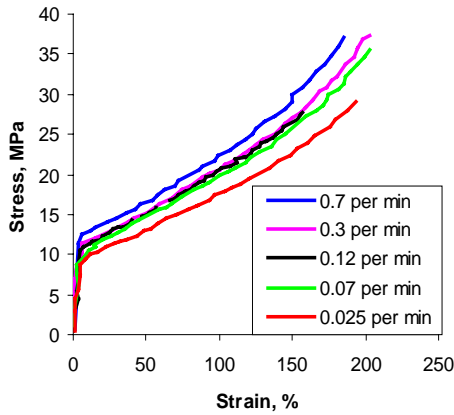


Figure 2. Nafion® 117 uniaxial loading test data

Table 1. Strain rate effect on Nafion® 117 yield strain and stress

Strain Rate (min <sup>-1</sup> )	Average Yield Strain (%)	Average Yield Stress (MPa)
0.7	8.05	12.66
0.3	8.3	11.57
0.12	8.775	10.59
0.07	9.13	10.50
0.025	9.45	9.946

Figure 3 illustrates the uniaxial loading results for the BPSH membranes. This figure shows a clear relationship between strain rate and strain at break. The higher the strain rate, the lower the breaking strain. The Young's modulus for BPSH, at  $940 \pm 20$  MPa, was much higher and more variable than that of N117. BPSH begins its ductile fracture at far lower strains than the brittle N117 fractures occur.

As mentioned in the Experimental Procedure section, the laser extensometer determined the strain for N117 and the crosshead displacement was used to determine the strain for BPSH. This necessary change makes the exact values of the two membranes' strain measurements incomparable. However, the trends illustrated in the graphs above still hold true. Strain rate has a much larger effect on strain at break in BPSH than in N117. Regardless of strain rate, BPSH begins its ductile fracture at far lower strains than the brittle N117 fractures occur.

### 3.2 Creep Compliance

Though creep tests on N117 ran from 10°C to 130°C, thermal contraction at lower temperatures

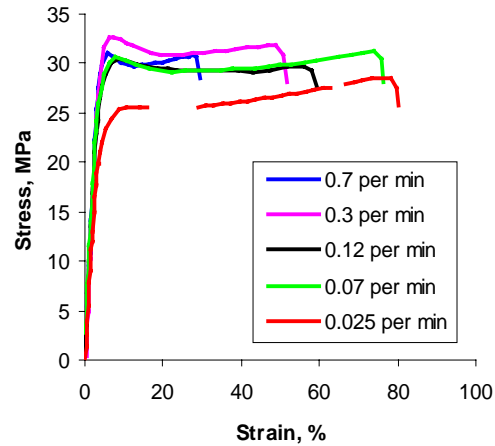


Figure 3. BPSH-35 uniaxial test data

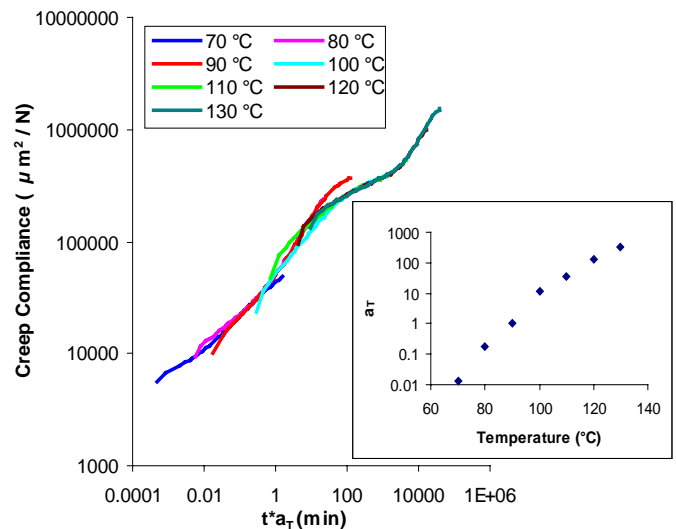


Figure 4. Nafion® 117 creep compliance master curve

tended to overwhelm the small stress used in the test, causing the sample to slowly contract instead of expand. The stress could not be increased, or else the sample would stretch farther at the higher temperatures than the instrument could measure. Since fuel cells typically run at roughly 60°C or more, the lower stress value was used. Figure 4 presents the master curve obtained from this test. The inset plot in Figure 4 shows the shift factor,  $a_r$ , used to generate the master curve.

For the same reasons as with the N117, BPSH creep tests could not produce accurate results at lower temperatures. Preload force values for the BPSH creep tests were the same as for the N117 tests. The data gathered was scattered and did not produce any

coherent master curve. Because of the high glass transition temperature ( $T_g$ ) of BPSH, it was tested at a temperature range above that of N117; however, this high temperature range initiated decomposition in the samples, probably because water absorption at high temperatures lowered the  $T_g$  more than initially anticipated. This decomposition most likely caused the scatter in the data.

#### 4. Conclusions

Uniaxial loading tests showed that for N117, higher strain rates lead to higher yield strains and yield stresses. Strain rate had no effect on the elongation at break for N117, but for BPSH, higher strain rates caused samples to fracture at lower strains. BPSH uniaxial test results illustrated no yield trends. N117 creep compliance data allowed for the creation of a reasonable master curve over the range of 70°C to 130°C. Due to some decomposition at high temperatures, BPSH creep data could not be used to produce a master curve. Additional mechanical testing is necessary to fully determine the possibility of replacing N117 with BPSH in fuel cell applications.

#### 5. Future Work

Many other tests could be used to further characterize these membranes' mechanical behavior. Any or all of the above experiments could test response to varying equivalent weights. Stress relaxation and/or uniaxial loading tests could be conducted at varying temperatures. Uniaxial loading behavior in the transverse direction, as well as biaxial loading tests, could also be useful. A series of recovery and/or compression tests might also be helpful. In addition, the delamination of the polymers from the platinum catalysts could be modeled, since this is also a cause for the failure of fuel cells.

#### Acknowledgements

The author owes this work to the assistance of Dr. Scott Case and Ms. Dan Liu for advising the research described herein during the 2004 Summer Undergraduate Research Program at Virginia Tech. He would like to express his gratitude to the National Science Foundation for funding through grant number DMR-0244141. Thanks also go to the laboratory

technicians in the Engineering Science and Mechanics Department for their time and patience and to Dr. Taigyoo Park for his generous assistance with the DMA machines. The author greatly appreciates the donations of samples from both DuPont and Dr. James McGrath of the Virginia Tech Chemistry Department.

#### References

1. Fowler, M.; Mann, R.; Amphlett, J.; Peppley, B.; Roberge, P., Incorporation of Voltage Degradation into a Generalized Steady State Electrochemical Model for a PEM Fuel Cell. *Journal of Power Sources* **2002**, 106, 274-283.
2. Hickner, M.; Ghassemi, H.; Kim, Y.S.; McGrath, J., Alternate Polymer Systems for Proton Exchange Membranes (PEMs). *Chemical Reviews* **2004**, 104, (10), 4587-4611.
3. Jiang, R.; Chu, D., Voltage-time Behavior of a Polymer Electrolyte Membrane Fuel Cell Stack at Constant Current Discharge. *Journal Power Sources* **2001**, 92, 193-198.
4. Wilson, M.S.; Garzon, F.; Sickafus, K.; Gottesfeld, S., Surface Area Loss of Supported Platinum in Polymer Electrolyte Fuel Cells. *Journal of the Electrochemical Society* **1993**, 10, 140.
5. St. Pierre, J.; Wilkinson, D.P.; Knight, S.; Bos, M., Relationships between Water Management, Contamination and Lifetime Degradation in PEFC. *Journal of New Materials Electrochemical Systems* **2000**, 3, 99-106.
6. Markovic, N.; Ross, P.N., New Electrocatalysts for Fuel Cells from Model Surfaces to Commercial Catalysts. *Cattech*: **2000**; (2), 110-126.
7. Tazi, B.; Savadogo, O., Parameters of PEM Fuel Cells Based on New Membranes Fabricated from Nafion, Silicotungstic Acid and Thiophene. *Electrochimica Acta* **2000**, 45, 4329-4339.
8. Kyu, T.; Eisenberg, A., *Mechanical Relaxations in Perfluorosulfonate Ionomer Membranes*. In *Perfluorinated Ionomer Membranes*; Eisenberg, A., Yeager, H., Eds.; A.C.S. Symposium Series 180; A.C.S. Publishing: 1982, p 79-110.
9. Brown, N., *Yield Behavior of Polymers*. In *Failure of Plastics*. Brostow, W., Corneliussen, R., Eds.; Hanser Publishers: 1989; p 104-10.